ORIGINAL PAPER

Journal of Anatomy | ANATOMICAL SOCIETY WILEY

A comparative anatomical and histological study on the presence of an apical splenic nerve in mice and humans

Cindy G.J. Cleypool ⬤ | **Claire Mackaaij** | **Suzanne A.M.W. Verlinde-Schellekens** | **Ronald L.A.W. Bleys**

Department of Anatomy, Division of Surgical Specialties, University Medical Center Utrecht, Utrecht University, Utrecht, the Netherlands

Correspondence
Cindy Cleypool, Center Utrecht, Division of Surgical Specialties: Departments of Anatomy, University Medical Center Utrecht, Utrecht University, Universiteitsweg 100, P.O. Box 85060, 3508 AB Utrecht, the Netherlands.
Email: c.g.j.cleypool@umcutrecht.nl

Abstract

The cranial pole of the mouse spleen is considered to be parasympathetically innervated by a macroscopic observable nerve referred to as the apical splenic nerve (ASN). Electrical stimulation of the ASN resulted in increased levels of splenic acetylcholine, decreased lipopolysaccharide-induced levels of systemic tumor necrosis factor alpha and mitigated clinical symptoms in a mouse model of rheumatoid arthritis. If such a discrete ASN would be present in humans, this structure is of interest as it might represent a relatively easily accessible electrical stimulation target to treat immune-mediated inflammatory diseases. So far, it is unknown if a human ASN equivalent exists. This study aimed to provide a detailed description of the location and course of the ASN in mice. Subsequently, this information was used for a guided exploration of an equivalent structure in humans. Microscopic techniques were applied to confirm nerve identity and compare ASN composition.

Six mice and six human cadavers were used to study and compare the ASN, both macro- and microscopically. Macroscopic morphological characteristics of the ASN in both mice and humans were described and photographs were taken. ASN samples were resected, embedded in paraffin, cut in 5 μm thin sections where after adjacent sections were stained with a general, sympathetic and parasympathetic nerve marker, respectively. Neural identity and nerve fiber composition was then evaluated microscopically.

Macroscopically, the ASN could be clearly identified in all mice and was running in the phrenicosplenic ligament connecting the diaphragm and apical pole of the spleen. If a phrenicosplenic ligament was present in humans, a similar configuration of potential neural structures was observed. Since the gastrosplenic ligament was a continuation of the phrenicosplenic ligament, this ligament was explored as well and contained white, potential discrete nerve-like structures as well which could represent an ANS equivalent. Microscopic evaluation of the ASN in mice and human showed that this structure did not represent a nerve, but most likely connective tissue strains.

White nerve-like structures, which could represent the ASN, were macroscopically observed in the phrenicosplenic ligament in both mice and human and in the gastrosplenic ligament in humans. The microscopic investigation did not confirm their neural identity and therefore, this study disclaims the existence of a parasympathetic ASN in both mice and human.

KEYWORDS
apical splenic nerve, cholinergic anti inflammatory pathway, neuro immunemodulation, splenic innervation

1 | INTRODUCTION

Splenic sympathetic nerves might represent a novel therapeutic target, as electrical stimulation of these nerves has shown to have beneficial anti-inflammatory effects in rodents (Kees et al., 2003; Komega et al., 2018; Vida et al., 2011). Upon stimulation, norepinephrine (NE) is released from these sympathetic nerves, followed by β2 adrenergic receptor activation on splenic CD4 positive T cells (Rosas-Ballina et al., 2011; Vida et al., 2011, 2017). These activated T cells produce and secrete acetylcholine (Ach) which ultimately inhibits the release of pro-inflammatory cytokines from activated macrophages through α7-nicotinic acetylcholine receptor signalling (Borovikova et al., 2000; de Jonge et al., 2005; Kox et al., 2009; Lu & Kwan, 2014). In addition to these sympathetic nerves, which run with the splenic artery, tracer studies in rats suggest the spleen is supplied by parasympathetic nerves as well (Buijs et al., 2008). These parasympathetic nerves were thought to enter the spleen at its poles as dissection of polar parts of the gastro splenic ligament abolished the presence of retrograde tracer in the dorsal motor nucleus (Buijs et al., 2008). The presence of such a parasympathetic nerve was confirmed in mice where a discrete nerve was macroscopically observed entering the spleen at its cranial pole (Guyot, et al., 2019). This nerve, by the authors referred to as the apical splenic nerve (ASN), contains primarily parasympathetic fibers and electrical stimulation of this nerve resulted in increased levels of splenic acetylcholine (Ach), decreased lipopolysaccharide (LPS) induced levels of systemic tumor necrosis factor alpha and mitigated clinical symptoms in a mouse model of rheumatoid arthritis (Guyot, et al., 2019). If such a discrete ASN would be present in humans, this structure could hold potential as a relatively easily accessible electrical stimulation target to treat immune-mediated inflammatory diseases. So far, the literature does not mention a discrete, macroscopic observable nerve entering the cranial pole of the human spleen. In order to investigate the existence of the ASN in humans, this study first aimed to macroscopically identify this nerve in mice and to describe its location and course. This information was then used for a guided exploration of an equivalent structure in humans. Microscopic techniques were additionally used to confirm nerve identity and to determine its composition.

2 | MATERIALS & METHODS

2.1 | Tissue resection

2.1.1 | Mice

Fixed cadavers of six 13 weeks old C57BL/6J male surplus mice were used. These mice were used for another experiment wherein they were anaesthetized with isoflurane and fixation was performed by means of transcardial perfusion with 2.5 ml of 4% paraformaldehyde (PFA). The right atrium was opened to drain excessive fluid. The abdomens were opened and the cadavers were additionally fixed *in toto* by immersion in 4% PFA for 24 h. After fixation, the cadavers were stored at 4°C in a 0.1 M phosphate buffer, pH 7.4, containing 15% sucrose (PBS/Sucrose) until further investigation. Further dissections were performed macroscopically and by using a stereomicroscope with both transmission and incident light (Leica EZ4, Nussloch, Germany). For the use of surplus cadaveric tissues, no ethics committee approval was required. The left halve of the liver was removed to get better access to the left upper abdominal quadrant containing the spleen, stomach and left-sided part of the diaphragm. While lifting the spleen and pulling it slightly downwards, the ASN became visible (Figure 1a). The stomach and spleen were positioned with needles securing a clear view of all relevant structures. After recording the course of the ASN *in situ*, the stomach, spleen, diaphragm and their connecting ligaments were removed *en block*, placed on a green transparent glass plate and studied with transmission light allowing better visualization of various structures (Figure 1b). Hereafter, the tip of the spleen, its suspending ligaments and the ASN were removed and stained *in toto* with haematoxylin according to a procedure previously described (Schurink et al., 2019) (Figure 1d). This staining provided better recognition of the ASN and the ligaments, and allowed complete trimming of these ligaments (Figure 1e). The tip of all spleens with its associated ASN were placed on 70% ethanol and further processed for microscopic evaluation. Vagus nerves, which show comparable macroscopic dimensions as the ASN and contain parasympathetic fibers were resected as well and used as controls.
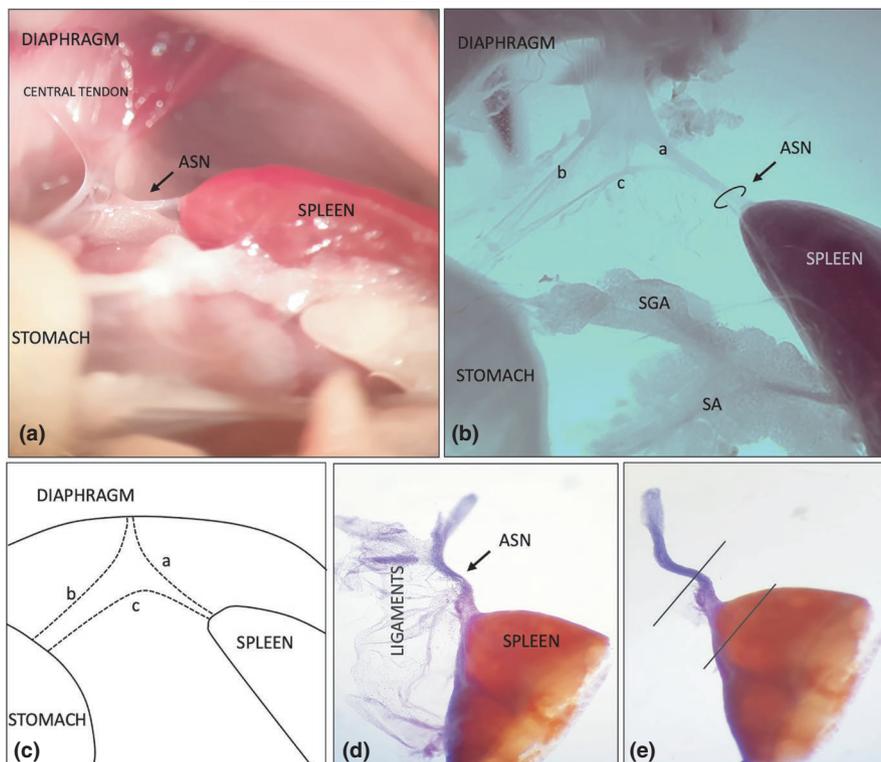
FIGURE 1 Apical splenic nerve in mice. (a) Ventral view on the upper left quadrant of the abdominal cavity with the spleen, diaphragm, stomach and connecting splenic ligaments *in situ*. (b) Ventral view on an isolated spleen, stomach, diaphragm and their connecting ligaments. White fibrous strands can be observed in the phrenicosplenic-, gastrophrenic-, and gastrosplenic ligaments (structures a, b and c respectively). (c) Schematic representation of the various observed white fibrous strands. (d) Hematoxylin-stained sample of the cranial tip of the spleen including some of its ligaments and the apical splenic nerve. (e) The same sample as shown in D. Trimming of the ligaments was performed to ensure microscopic slides to contain the apical splenic nerve only. Black lines illustrate the location of the apical splenic nerve and spleen slides as obtained from each mouse

2.1.2 | Humans

Seven human cadavers were provided for this study: four female and three male cadavers with a median age of 93 years at death (interquartile range: 79–98). All bodies entered the Anatomy department of the University Medical Centre Utrecht, the Netherlands, through a body donation program. Informed consent was obtained during life, allowing the use of these bodies for educational and research purposes. Whole-body preservation was accomplished by arterial perfusion of approximately 10 L of 3% PFA via the femoral artery. The abdomens were opened, the left halves of the livers were removed and the spleen, stomach, diaphragm and suspending splenic ligaments, being the phrenicosplenic ligament (PSL) and gastrosplenic ligament (GSL), were identified. The presence of ASN-like structures was recorded. In order to further microscopically assess the neural identity of observed ASN-like structures, the PSLs, which is the ligament containing the ASN in mice (as shown in the current study) was isolated as a whole. In humans, the PSL was only present in 2/6 cadavers and since the GSL is a caudal continuation of the PSL, it was decided to additionally study the GSL as well. The GSL was sampled at three different locations; at the cranial border of the ligament (or at the border of the GSL with the PSL if a PSL was

present) and at locations that showed clear white fibrous strands, which could potentially represent nerves. In addition, one spleen and its associated PSL and GSL was isolated as a whole, allowing microscopic evaluation of these ligaments *in toto* in case discrete neural structures were missed out in the resected parts. All samples were placed on 70% ethanol and further prepared for microscopic evaluation as following.

2.2 | Tissue sample preparation for microscopic investigation

All samples were processed for paraffin embedding by placing them in increasing percentages of ethanol, xylene and paraffin. Tissues were then embedded in paraffin in such a way that the cutting plane would be perpendicular to the course of presumably neural structures. All resected nerves, spleens (both mice) and ligaments (humans) were cut in 5-μm thick sections on a microtome (Leica 2050 Super Cut, Nussloch, Germany) whereas the human ligament *in toto* was cut in 10 μm thick sections on a microtome (Leica Tetrander, Nussloch, Germany). All sections were placed on glass slides, air-dried and subsequently heat fixed for 2 h on a slide drying table of 60°C (Medax,

14801, Kiel, Germany). Mouse ASN and spleen slides (the latter containing a substantial amount of hilar and parenchymal tissue) were single stained with antibodies raised against protein gene product 9.5 (PGP9.5) and tubulin III (Tub III) to identify neural structures in general, and antibodies against tyrosine hydroxylase (TH) and choline acetyl transferase (ChAT), to analyse whether neural structures were composed of sympathetic or parasympathetic nerve fibers respectively. Human splenic ligament slides (both PSL and GSL) were stained with PGP9.5 to verify the neural identity of the macroscopically observed ASN-like structures. Details on all immune histochemical staining procedures can be found in the following paragraph.

2.2.1 | Immunohistochemical staining (TubIII, ChAT TH)

All slides were deparaffinized and rehydrated, followed by 20 min of antigen retrieval in 95°C citrate buffer on a hot plate. After washing in Tris-buffered saline (TBS) with 0.05% tween (TBS/Tween), mice and human sections were pre-incubated for 10 min with 5% normal mouse or human serum respectively. After preincubation, sections were incubated with primary antibodies in TBS with 3% bovine serum albumin (see Table 1 for technical details). Following incubation, sections were washed with TBS/Tween and incubated for 30 min at room temperature (RT) with secondary antibodies being undiluted Brightvision Poly-Alkaline phosphatase (see Table 1 for specific details) After incubation, all sections were washed with TBS and incubated with Liquid Permanent Red (LPR) (DAKO, Glostrup, Denmark) for 10 min. Subsequently, tissue sections were washed with distilled water and counterstained with haematoxylin, air-dried at 60°C for 90 min, and cover-slipped using Entellan (Merck, Darmstadt, Germany). Mouse spleen and vagus nerve sections of the same mice were used as positive controls whereas for human samples, intrinsic paravascular nerves served as positive controls. Negative controls were obtained by incubation of both mice and human slides with TBS-3% BSA without primary antibody. All slides were evaluated using bright field microscopy.

2.3 | Image acquisition

Macroscopic images and more detailed images of dissections (through a stereomicroscope) were obtained using a smart phone camera (Samsung S9, Seoul, South Korea). Brightfield microscopic single and stitched overview images were captured at various magnifications using a DM6 microscope with a motorized scanning stage, a DFC7000 T camera and LASX software (all from Leica, Nussloch, Germany).

3 | RESULTS

3.1 | Macroscopic observations

3.1.1 | Mice

All mice showed a whitish neural plexus like structure in the left upper quadrant of the abdomen cranial to the spleen and stomach, interconnecting the spleen, stomach and the diaphragm (Figure 1a). The relevant tissues (stomach, spleen, diaphragm and their interlinking ligaments with its neural plexus like structures) were removed *en block* and placed on a dark green glass plate and studied under the stereomicroscope using only transmission light. This allowed for better determination of all relevant structures (Figure 1b). Three separate white strands could be distinguished in the plexus-like structure. The first strand was connecting the cranial pole of the spleen with the connective tissue of the central tendon of the diaphragm (Figure 1b structure a). From the same location at the diaphragm, a similar structure, which partly runs parallel with structure (a), could be observed running towards the fundus of the stomach (Figure 1b structure b). A third strand was observed running between the stomach and the cranial pole of the spleen (Figure 1b structure c). The spleen is attached to the stomach and diaphragm by various ligaments, which were composed of a double sheet of peritoneum. These ligaments were very thin and difficult to observe both macro—and stereomicroscopically. Only if the incident light of the stereomicroscope hit the ligaments from the right angle, these ligaments became shiny and recognizable. The splenorenal ligament attached the spleen to the dorsal body wall and contained the splenic artery with its terminal branches. The GSL is positioned ventrally with respect to the splenorenal ligament and connected the spleen to the stomach and contained a short gastric artery and structure c (Figure 1b). The PSL connected the spleen to the diaphragm and contained structure a and the final part of structure c (Figure 1b), which together formed the presumably ASN.

TABLE 1 Technical specifications of used antibodies

	Host + clone	Vendor	Order #	Dilution, incubation time and temperature
TH	Rabbit Polyclonal	PelFreez (Rogers, USA)	P40101	1:400, o.n., RT
PGP9.5	Rabbit Polyclonal	Dako (Glostrup, Denmark)	Z5116	1:2000, 48 h, 4°C
ChAT	Goat polyclonal	Millipore (Burlington, USA)	AB144P	1:50, o.n., 4°C
TubIII	Mouse mono IgG2a	R&D systems (Minneapolis, USA)	MAB1195	1:10.000, 60 min, RT

3.1.2 | Humans

In contrast to the mouse, in humans, the suspending splenic ligaments are much thicker and therefore clearly recognizable. Since the ASN, as shown in mice, was positioned within the PSL, the latter was explored for the presence of discrete macroscopically visible nerves in humans. In 2/6 cadavers a PSL was present. This ligament was observed running from the diaphragm to the cranial tip of the spleen (Figure 2a,b) and contained white fibrous strands which ran from the central tendon of the diaphragm to the tip of the spleen (Figure 2a,e). A clearly observable GSL was present in all cadavers and connected the fundus and part of the greater curvature of the stomach to the spleen. Comparable to the greater omentum in humans, the GSL contains a significant amount of adipose tissue making it difficult to distinguish discrete structures. However, when stretched, white strands could be observed running from the surface of the stomach to the hilum of the spleen (Figure 2d).

3.2 | Microscopic observations

3.2.1 | Mice

All ASNs were composed of a homogenous tissue mass, enclosed by a covering mesothelium (Figure 3a,d). None of the ASNs showed immunoreactivity (IR) for the general nerve markers PGP9.5 and TubIII (Figure 3a,b) nor for the sympathetic nerve marker TH (Figure 3c). ChAT staining of the ASN showed a homogenous light pink staining comparable to the general background staining as observed in e.g. adipose and connective tissue (Figure 3d,h,l,p).

All neural controls showed the following expected staining patterns. The splenic hilum contained a SA with peri and paravascular nerves (Figure 2e,f) which were predominantly sympathetic of nature (Figure 2g). In the splenic parenchyma, fine sympathetic nerves were observed to run with vascular structures and occasionally branched off and travelled further into the parenchyma (Figure 2i–k). The vagus nerve showed clear staining for both general nerve markers and was composed of a few sympathetic and a significant amount of parasympathetic nerve fibers (Figure 3o,p). Furthermore, strong ChAT-IR was observed in cellular structures that were primarily present in the splenic red pulp and which occasionally interspersed the white pulp.

3.2.2 | Humans

A few small discrete nerves were observed in the connective tissue of both the PSLs and GSLs (Figure 4), but never represented dimensions complying with the macroscopically observed ASN-like
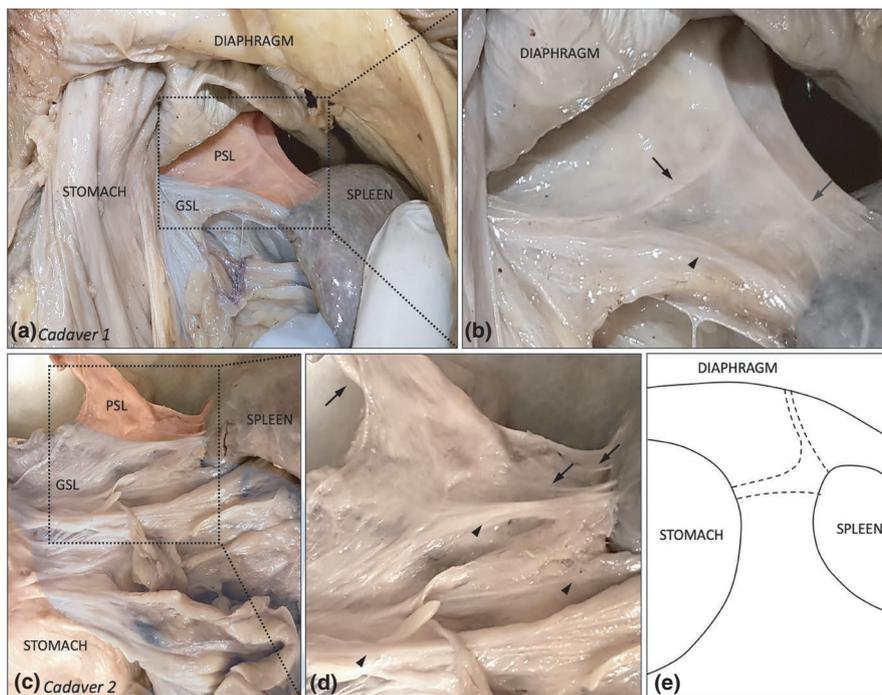
FIGURE 2 Apical splenic nerve-like structures in humans. (a) Ventral view on the upper left quadrant of the abdominal cavity of cadaver 1. The spleen, diaphragm, stomach and connecting ligaments can be observed *in situ*. (b) Close up of the ligaments of Figure A, showing white fibrous strands which might represent equivalent structures to the once observed in mice (Figure 1b). (c) Ventral view on the upper left quadrant of the abdominal cavity of cadaver 2. (d) Close up of the ligaments of Figure A, showing white fibrous strands which might represent equivalent structures to the once observed in mice (Figure 1b). (e) Schematic representation of the various observed white fibrous strands. Arrows: white strand-like structures running between the diaphragm and the spleen and fundus of the stomach. Arrow heads: white nerve-like structures running between the stomach and the spleen
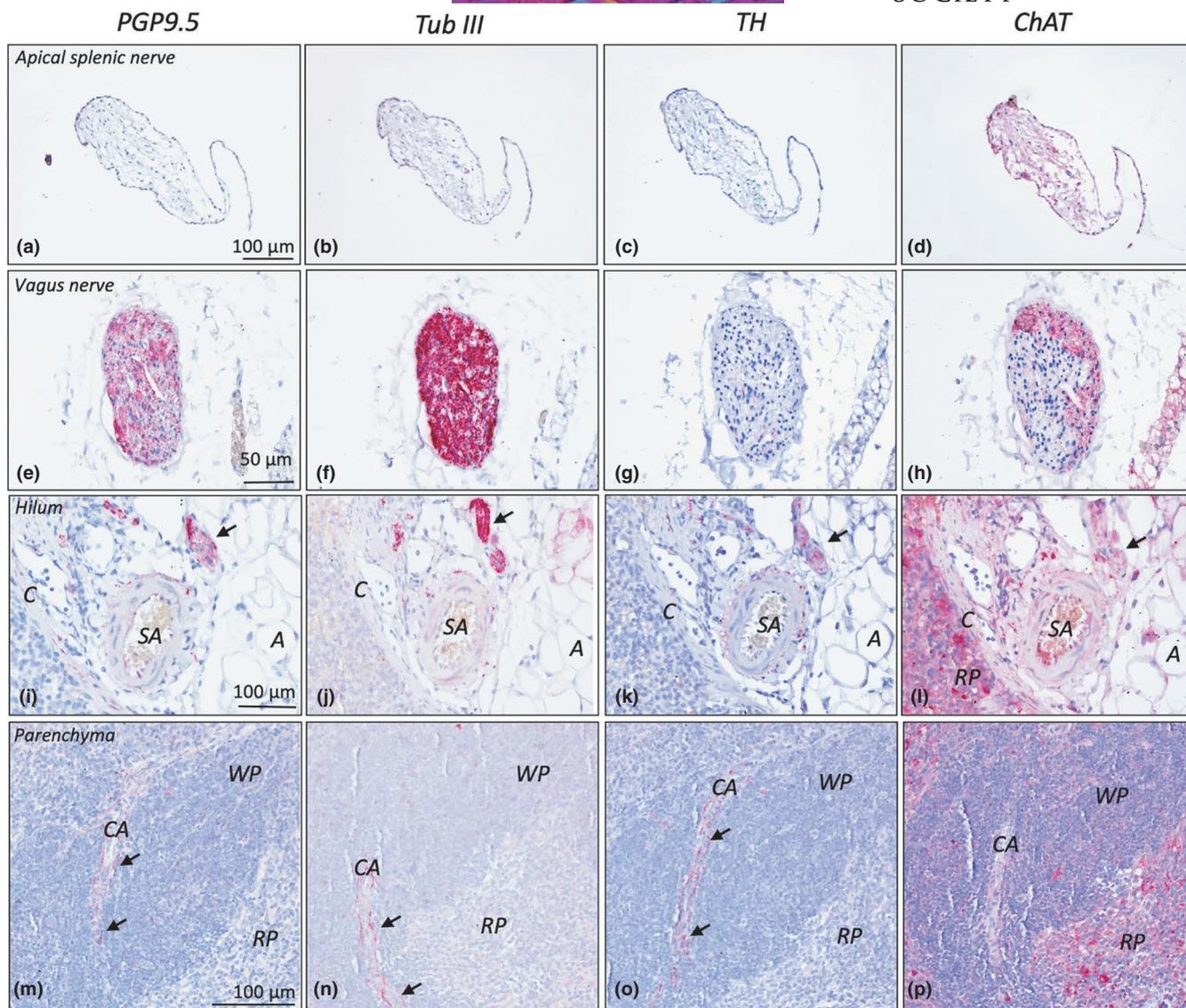
FIGURE 3 Microscopic images of the apical splenic nerve in mice stained with various nerve markers. The apical splenic nerve and various control tissues were stained with general nerve markers (PGP9.5 and TubIII) and a sympathetic (TH) and parasympathetic nerve marker (ChAT), all visualized by a pink chromogen. (a–d) Apical splenic nerve. Based on the absence of staining with general nerve markers it can be concluded that the ASN does not contain nerve fibers. ChAT staining results are doubtful, but based on staining patterns in the control tissues it can be concluded that this marker shows strong immune reactivity (IR) with non-neuronal tissues (immune cells) and weak IR for a few other tissues such as connective tissue and smooth muscle cells (vessel walls, capsule). (e–h) Vagus nerve. The vagus nerve is composed of a few sympathetic (TH-IR) nerve fibers, a substantial amount of parasympathetic (ChAT-IR) fibers. The fibers that remain most likely represent afferent fibers. (i–l) Splenic hilum. At the splenic hilum, splenic artery branches enter the spleen. These arteries are accompanied by sympathetic (TH-IR) nerves. A significant number of ChAT-IR cells are present in the spleen. These cells predominantly reside in the red pulp, but can be observed inside blood vessels and in between the connective tissue of the hilum. (m–p) Splenic parenchyma. Sympathetic (TH-IR) nerves run with arteries deeper into the splenic parenchyma. A significant number of ChAT-IR cells are present in the spleen. These cells predominantly reside in the red pulp. A, Adipocytes; CA, Central artery; RP, Red pulp; SA, Splenic artery; WP, White pulp; Arrow, Nerve

structures shown in Figure 2b. Furthermore, moderate-sized nerves were observed in association with the short gastric arteries (SGA) (Figure 4c–f). Again, these nerves could not be observed by the naked eye and could not represent macroscopically observable ASN-like structures as shown in Figure 3d.

4 | DISCUSSION

Although the presence of noradrenergic nerves in the spleen in various species is well established (Bellinger et al., 1987, 1992; Hoover et al., 2017; Murray et al., 2017; Verlinden et al., 2018), the
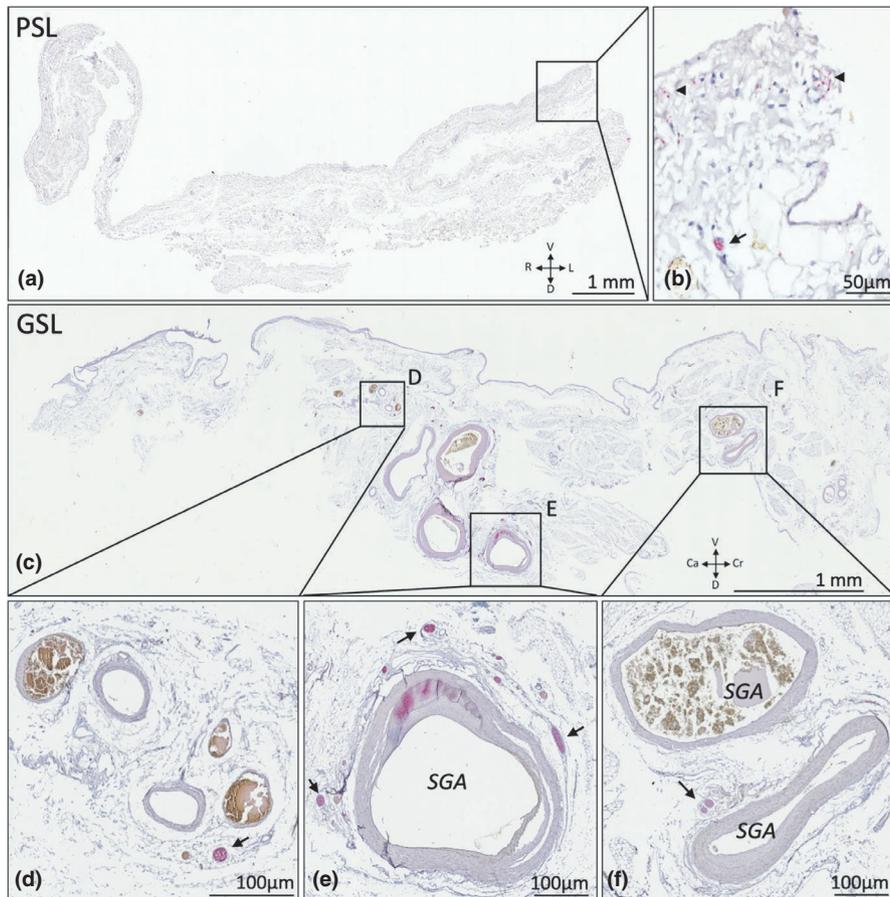
FIGURE 4 Microscopic images of splenic ligaments with observed apical splenic nerve-like structures in humans. Both ligaments are stained with a general nerve marker (PGP9.5) which is visualized by a pink chromogen. (a, b) Overview image of one of the two phrenicosplenic ligaments (PSL). The ligament is primarily composed of connective tissue with scattered small blood vessels and fine nerves. If nerve bundles were present, these were sparse and small and did not represent the macroscopic observed nerve-like structures as presented in Figure 2b. (c–f) Overview image of the *in toto* studied gastrosplenic ligament (GSL). Various short gastric arteries and smaller vascular structures can be observed (some blood vessels are filled with blood which has a brownish appearance in these slides). Comparable to the PSL, the GSL was composed of connective tissue. Scattered throughout the ligament fine nerves could be observed (the relatively low magnifications do not allow to observe these). Surrounding the short gastric arteries (SGA), various paravascular nerve bundles can be observed. These, however, do not represent the macroscopic observed nerve-like structures as presented in Figure 2d. Arrow heads, Scattered fine nerves; Arrows, Small nerve bundles

presence of cholinergic nerves is still under debate. Various studies disclaim the existence of splenic parasympathetic innervation (Bellinger et al., 1993; Cano et al., 2001; Hoover, 2017; Verlinden et al., 2018), whereas other reported opposite observations (Buijs et al., 2008; Gautron et al., 2013). With the recent discovery of the ASN, a macroscopic observable nerve of cholinergic nature as shown by immune histochemical stainings and electrical stimulation, this debate might have come to an end. However, the current study shows that the structure that is referred to as the ASN in mice, is mainly composed of connective tissue and does not represent a macroscopic observable nerve. This significant discrepancy could be explained by inaccurate inclusion of non-ASN tissue in the current study. This however seems unlikely as prior to resection of the presumably ASN, the location, appearance and course of what was considered to represent this structure was confirmed via personal communication with the corresponding author of

the study of Guyot et al (Guyot et al., 2019). Furthermore, by applying whole mount hematoxylin staining (Figure 1d,e), all irrelevant structures were trimmed in order to avoid obscurity of the results. Secondly, it was questioned whether the immunohistochemical staining results of the current study were erroneous. To make sure that the observations were trustworthy, several tissues with known noradrenergic and cholinergic neural staining patterns were included as controls and included the vagus nerve and hilar and parenchymal splenic tissue. All controls showed expected staining patterns, confirming staining accuracy for general, sympathetic and cholinergic nerve markers. It was however noticed, that in addition to nerve fibers as observed in the vagus nerve, ChAT antibodies showed strong IR in various non-neuronal structures such as red pulp-associated immune cells, blood vessel content and adipocytes, and, showed light IR in connective tissue rich structures such as the capsule, trabeculae and vessel walls.

These non-neuronal ChAT-IR patterns might explain the observations in ChAT-stained ASN slides of Guyot et al. Furthermore, light sheet images of this author did not convincingly show a discrete ChAT-IR nerve at the tip of the spleen and in general, ChAT-IR was observed in a fragmented pattern, which is not suggestive for nerves. The fragmented pattern was observed at various locations in the light sheet imaged spleen and might be better explained as ChAT-IR immune cells, since these are largely present as shown in splenic parenchyma slides of the current study.

Thus, from an anatomical point of view the results of the current study cast doubt on the existence of an ASN. However, from a functional point of view, the 'ASN' (from now on placed between quotation marks due to its disclaimed existence), does represent an interesting structure as electrical stimulation of this structure resulted in increased levels of splenic NE and Ach, whereas stimulation of splenic artery associated nerves resulted in splenic NE increase only. Now that the neural identity of the 'ASN' is in doubt and this increase in splenic neurotransmitters (both NE and Ach) could not be attributed to its nerve fibers, could these observations be explained otherwise? Leakage of electrical current could hypothetically result in stimulation of splenic artery associated sympathetic nerves and hence explain the increase of splenic NE levels. The source of non-neuronal Ach could then be explained by subsequent activation of $CD4^+$ T cells. However, Guyot et al., showed that this increase of Ach levels was independent to both T cells and adrenergic signaling. These observations lead the authors to conclude that Ach could only be derived from the cholinergic fibers of the ASN, thereby strengthening the assumption of its existence. However, ChAT expression has been observed in other immune cells such as B cells (Gautron et al., 2013), dendritic cells and macrophages (Fuji et al., 2017). ChAT-IR cells in the spleen are not a rare entity, but moreover represented a large cell population in normal spleens, as can be observed in the splenic parenchymal control samples of the current study. Moreover, a significant portion of these ChAT-IR cells did not display a typical lymphocyte morphology or overlapping distribution patterns with T cells (unpublished data, Cleypool), supporting the presence of a significant number of alternative cellular Ach sources. Could the 'ASN' transmit electrical current towards the spleen, and moreover, directly activate alternative Ach sources? The current study showed that the 'ASN' in mice was composed of homogenous connective tissue positioned between two layers of mesothelium, together constituting the PSL. It is known, that if physiological forces are applied to connective tissue, collagen fibrils will align into orientated bundles (Kalson et al., 2013), a process which might have occurred in the PSL and explain the presence of discrete white fibrous strands, including the 'ASN' (Figure 1). Collagen fibrils show electrical conductivity (Bardelmeyer, 1973) and 'ASN' stimulation might result in the transmission of electrical signals to, for example, the splenic capsule. If and how electrical signals could then be further transmitted to, for example, cholinergic B cells, macrophages or dendritic cells remains unknown. However, the splenic capsule, which contains a significant amount of smooth muscle cells, forms a continuous structure with the reticular framework. This framework represents the splenic connective tissue scaffold and is composed of collagen fibers enveloped by myofibroblasts; fibroblasts with smooth muscle cell-like characteristics. Smooth muscle cells are known to be electrically coupled via gap junctions and can conduct action potentials from one cell to another. If such coupling electrically conjoins the splenic capsule and the reticular fiber network, electrical stimulation of the 'ASN' and hence the splenic capsule might activate the reticular framework. Since myofibroblasts of this framework can release various chemokines and cytokines, express chemokine receptor ligands, and, is involved in guided migration of immune cells, regulation of immune function (Perez-Shibayama et al., 2019; Zhao et al., 2015), activation of this framework can have significant effects on the immune response.

Although the ASN does not represent a neural structure, its intermediate role in the activation of an Ach mediated, T cell and adrenergic receptor-independent anti-inflammatory mechanism is intriguing and triggers further research. This research might include mechanisms that activate the release of intrasplenic Ach from, for example, macrophages and dendritic cells, and, connective and splenic tissue transmission routes of electrical current and excitability of the reticular network.

5 | CONCLUSION

Microscopic evaluation of the ASN in mice and humans dismissed its neural identity, thereby casting doubt on its existence. The anti-inflammatory effect upon electrical stimulation of this non-neural structure in mice points out that our understanding of the regulation of the splenic immune response is incomplete.

ORCID
Cindy G.J. Cleypool https://orcid.org/0000-0003-4993-3736

REFERENCES
Bardelmeyer, G.H. (1973) Electrical conduction in hydrated collagen. I. Conductivity mechanisms. *Biopolymers*, 12(10), 2289–2302.

Bellinger, D.L., Ackerman, K.D., Felten, S.Y. & Felten, D.L. (1992) A longitudinal study of age-related loss of noradrenergic nerves and lymphoid cells in the rat spleen. *Experimental Neurology*, 116, 295–311.

Bellinger, D.L., Felten, T.J., Collier, T.J. & Felten, D.L. (1987) Noradrenergic sympathetic innervation of the spleen: IV. Morphometric analysis in adult and aged F344 rats. *Journal of Neuroscience Research*, 18(1), 55–63.

Bellinger, D.L., Lorton, D., Hamill, R.W., Felten, S.Y. & Felten, D.L. (1993) Acetylcholinesterase staining and choline acetyltransferase

activity in the young adult rat spleen: lack of evidence for cholinergic innervation. *Brain, Behavior, and Immunity*, 7(3), 191–204.

Borovikova, L.V., Ivanova, S., Zhang, M., Yang, H., Botchkina, G.I., Watkins, L.R. et al. (2000) Vagus nerve stimulation attenuates the systemic inflammatory response to endotoxin. *Nature*, 405(6785), 458–462.

Buijs, RuudM, Van Der Vliet, J., Garidou, M.-L., Huitinga, I. & Escobar, C. (2008) Spleen vagal denervation inhibits the production of antibodies to circulating antigens. *PLoS One*, 3(9), 1–8.

Cano, G., Sved, A.F., Rinaman, L., Rabin, B. & Card, J.P. (2001) Characterization of the central nervous system innervation of the rat spleen using viral transneuronal tracing. *Journal of Comparative Neurology*, 439(1), 1–18.

de Jonge, W.J., van der Zanden, E.P., The, F.O., Bijlsma, M.F., van Westerloo, D.J., Bennink, R.J. et al. (2005) Stimulation of the vagus nerve attenuates macrophage activation by activating the Jak2-STAT3 signaling pathway. *Nature Immunology*, 6(8), 844–851.

Fujii, T., Mashimo, M., Moriwaki, Y., Misawa, H., Ono, S., Horiguchi, K. et al. 2017. Expression and function of the cholinergic system in immune cells. *Frontiers in Immunology*, 8, 1085.

Gautron, L., Rutkowski, J.M., Burton, M.D., Wei, W., Wan, Y. & Elmquist, J.K. (2013) Neuronal and nonneuronal cholinergic structures in the mouse gastrointestinal tract and spleen. *Journal of Comparative Neurology*, 521(16), 3741–3767.

Guyot, M., Simon, T., Panzolini, C., Ceppo, F., Daoudlarian, D., Murris, E. et al. (2019) Apical splenic nerve electrical stimulation discloses an anti-inflammatory pathway relying on adrenergic and nicotinic receptors in myeloid cells. *Brain, Behavior, and Immunity*, 80(March), 238–246.

Hoover, D.B. (2017) Cholinergic modulation of the immune system presents new approaches for treating inflammation. *Pharmacology and Therapeutics*, 179, 1–16.

Hoover, D.B., Brown, T.C., Miller, M.K., Schweitzer, J.B. & Williams, D.L. (2017). Loss of sympathetic nerves in spleens from patients with end stage sepsis. *Frontiers in Immunology*, 8, 1–10.

Kalson, N.S., Starborg, T., Yinhui, L.U., Mironov, A., Humphries, S.M., Holmes, D.F. et al. (2013) Nonmuscle myosin II powered transport of newly formed collagen fibrils at the plasma membrane. *Proceedings of the National Academy of Sciences*, 110(49), E4743–E4752.

Kees, M.G., Pongratz, G., Kees, F., Schölmerich, J.U. & Straub, R.H. (2003) Via β-adrenoceptors, stimulation of extrasplenic sympathetic nerve fibers inhibits lipopolysaccharide-induced TNF secretion in perfused rat spleen. *Journal of Neuroimmunology*, 145(1–2), 77–85.

Komega, E.N., Stephen Farmer, D.G., Brooks, V.L., McKinley, M.J., McAllen, R.M. & Martelli, D. (2018). Vagal afferent activation suppresses systemic in flammation via the splanchnic anti-inflammatory pathway. *Brain, Behavior, and Immunity*, 73(December 2017), 441–449.

Kox, M., van Velzen, J.F., Pompe, J.C., Hoedemaekers, C.W., van der Hoeven, J.G. & Pickkers, P. (2009) GTS-21 inhibits pro-inflammatory cytokine release independent of the toll-like receptor stimulated via a transcriptional mechanism involving JAK2 activation. *Biochemical Pharmacology*, 78(7), 863–872.

Lu, B., Kwan, K., Levine, Y.A., Olofsson, P.S., Yang, H., Li, J. et al. (2014) A7 nicotinic acetylcholine receptor signaling inhibits inflammasome activation by preventing mitochondrial DNA release. *Molecular Medicine*, 20(1), 350–358.

Murray, K., Godinez, D.R., Brust-Mascher, I., Miller, E.N., Gareau, M.G. & Reardon, C. (2017) Neuroanatomy of the spleen: mapping the relationship between sympathetic neurons and lymphocytes. *PLoS One*, 12(7), 1–17.

Perez-Shibayama, C., Gil-Cruz, C. & Ludewig, B. (2019) Fibroblastic reticular cells at the nexus of innate and adaptive immune responses. *Immunological Reviews*, 289(1), 31–41.

Rosas-Ballina, M., Olofsson, P.S., Ochani, M., Valdes-Ferrer, S.I., Levine, Y.A., Reardon, C. et al. (2011) Acetylcholine-synthesizing T cells relay neural signals in a vagus nerve circuit. *Science*, 334(6052), 98–101.

Schurink, B., Cleypool, C.G.J. & Bleys, R.L.A.W. (2019) A rapid and simple method for visualizing milky spots in large fixed tissue samples of the human greater omentum. *Biotechnic & Histochemistry*, 94(6), 1–6.

Verlinden, T.J.M., Van Dijk, P., Hikspoors, J., Herrler, A., Lamers, W.H. & Eleonore Köhler, S. (2018). Brain, behavior, and immunity innervation of the human spleen : a complete hilum-embedding approach. *Brain Behavior and Immunity*, 77, 1–9.

Vida, G., Peña, G., Deitch, E.A. & Ulloa, L. (2011) Alpha7-cholinergic receptor mediates vagal induction of splenic norepinephrine. *Journal of Immunology*, 186(7), 4340–4346.

Vida, G., Peña, G., Kanashiro, A., Thompson-Bonilla, M.D.R., Palange, D., Deitch, E.A. et al. (2017) B2-adrenoreceptors of regulatory lymphocytes are essential for vagal neuromodulation of the innate immune system. *The FASEB Journal*, 25(12), 4476–4485.

Zhao, L., Liu, L., Guo, B.O. & Zhu, B.O. (2015) Regulation of adaptive immune responses by guiding cell movements in the spleen. *Frontiers in Microbiology*, 6, 1–6.